The last *r* locus unveiled: T4 RIII is a cytoplasmic co-antiholin

Yi Chen [a,b] and Ry Young [a,b#]

Department of Biochemistry and Biophysics, Texas A&M University, College Station, Texas [a]

Center for Phage Technology, Texas A&M University, College Station, Texas [b]

Running title: T4 RIII is a co-antiholin

#Address correspondence to Ry Young, ryland@tamu.edu, Phone: 979-845-2087, Fax: 979-862-4718

Abstract

The latent period of phage T4, normally ~25 min, can be extended indefinitely if the infected cell is super-infected after 5 min. This phenomenon, designated as lysis inhibition (LIN), was first described in the 1940s and genetically defined by mutations in diverse T4 *r* genes. RI, the main effector of LIN, was shown to be secreted to the periplasm where, upon activation by super-infection with a T-even virion, it binds to the C-terminal periplasmic domain of the T4 holin T, and blocks its lethal permeabilization of the cytoplasmic membrane. Another *r* locus, *rIII*, has been the subject of conflicting reports. Here we show that RIII, an 82 amino acid protein, is also required for LIN in both *Escherichia coli* B strains and K-12 strains. In T4Δ*rIII* infections, LIN was briefly established but was unstable. The overexpression of a cloned *rIII* gene alone impeded T-mediated lysis temporarily. However, co-expression of *rIII* and *rI* resulted in a stable LIN state. Bacterial two-hybrid assays and pull-down assays showed that RIII interacts with the cytoplasmic N-terminus of T, which is a critical domain for holin function. We conclude that RIII is a T4 antiholin which blocks membrane hole-formation by directly interacting with the holin. Accordingly, we propose an augmented model for T4 LIN that involves the stabilization of a complex of three proteins in two compartments of the cell: RI interacting with the C-terminus of T in the periplasm and RIII interacting with the N-terminus of T in the cytoplasm.

47 **Importance**

48 Lysis inhibition is a unique feature of phage T4 in response to environmental conditions,
49 effected by the antiholin RI, which binds to the periplasmic domain of the T holin and
50 blocks its hole-forming function. Here we report that T4 gene *rIII* encodes a cytoplasmic
51 antiholin which inhibits holin T, together with the main antiholin RI, by forming a complex
52 of three proteins spanning two cell compartments.

53

54 **Introduction**

55 The *r* genes of the T-even phages, first identified by laboratories of the Phage
56 Group in the 1940s (1, 2), have a special place in the history of molecular biology.
57 Detailed studies of the first three loci discovered, - *rI*, *rIIAB*, and *rIII*, - were
58 foundational in working out the fundamentals of inheritance, the genetic code, mutation,
59 recombination, DNA repair, and gene structure (3-7). These mutable loci were originally
60 discovered by their distinctive plaque morphology: large, clear, sharply-defined plaques,
61 easily distinguished from the small, fuzzy-edged turbid plaques of the parental phages
62 (1). The "*r*" designation meant "rapid lysis", which refers to the observation that the
63 mutant phages isolated from the r-type plaques caused rapid, culture-wide lysis at ~25
64 min after infection, whereas cultures infected with the parental phages continued to
65 increase in mass and accumulated progeny virions intracellularly for hours, in a state
66 called "lysis inhibition"(LIN)(8). In the ensuing decades, more loci were assigned as *r*
67 genes based on mutant plaque phenotypes; at one point, there were *r* genes numbered
68 up to *rVI* that were assigned map positions (9, 10). In 1998, Paddison *et al*. (11)

reviewed this field and concluded that only *rI*, *rIII* and *rV* were directly involved in LIN, with the other genes causing lysis phenotypes through indirect physiological pathways. The *rV* mutants were shown to be missense alleles of gene *t*, which encodes T, the holin of phage T4 (12). Holins are the master lysis control proteins of Caudovirales (13), acting to terminate the infection cycle by permeabilizing the cytoplasmic or inner membrane (IM) at a programmed time. It followed that the simplest operational model to explain the involvement of the remaining loci associated with direct LIN defects, *rI* and *rIII*, would be that the RI and RIII proteins were required to inhibit the lethal function of T and thus establish the LIN state (9, 11).

More recent studies on T and RI have confirmed aspects of this operational model for LIN and provided molecular details for the lysis pathway of T4 (14-16). Like other holins, including the well-studied S105 holin of phage lambda, the T holin accumulates harmlessly in the host IM until it suddenly forms lethal, micron-scale membrane lesions at an allele-specific time. This event, which is defined as holin triggering, results in the escape of cytoplasmic endolysin E (product of gene *e*) (13) into the periplasm, where it rapidly degrades the cell wall. In turn, the loss of cell wall activates the spanin complex (product of *pseT.2* and *pseT.3*)(17), which then disrupts the outer membrane (OM) and completes the release of the progeny. In single infections, T4 completes this three-step pathway in ~25 min (1). However, if the T4-infected cells are super-infected by other T4 (or T-even phages) after the first five minutes of the infection cycle, LIN is imposed (18). There has been progress on the molecular basis of LIN (15, 19-21). While most holins have two or more transmembrane domains (TMDs) and only short soluble loops connecting them (13), the T holin has a

unique structure, with only a single TMD and significant N- (34 aa) and C-(163 aa) terminal cytoplasmic and periplasmic domains, respectively (15, 22) **(Fig. 1)**. Moreover, the RI protein was shown to have a SAR (signal anchor release) domain, which is a TMD that can escape from the membrane (19). By virtue of this domain, RI is secreted initially as a membrane-tethered periplasmic protein and then releases into the periplasm where, in single infections, it is degraded rapidly (19, 20). However, under LIN conditions, (i.e., when there is superinfection with a second T4 phage particle), RI is stabilized and accumulates in the periplasm, where it forms an equimolar complex with the cytoplasmic domain of T and inhibits triggering, thus imposing the LIN state. Additionally, if the SAR domain of RI is replaced by a cleavable Signal Peptidase I signal sequence, the processed RI protein over-accumulates in the periplasm in a stable, mature form, forms the complex with T and imposes LIN without requiring the superinfection activation (19, 20).

Because RI is a specific inhibitor of T, it is formally a member of a diverse class of proteins designated as antiholins (23-26). Moreover, since RI inhibits T only under certain physiological conditions, it is the only antiholin known that transduces environmental information to effect real-time control of holin function and thus the length and fecundity of the phage infection cycle (21). However, despite these conceptual and mechanistic advances with T and RI, the genetic basis of the LIN phenomenon remains incomplete, some decades after the genetics of the *r* genes were first published, because no role has been found for *rIII* (1, 3). Although it was reported that RIII was not required for LIN on some K-12 strains (6), *rIII* shares with *rI* the feature that neither locus can suppress *t* lysis-null mutations and both loci are transcribed from both early

and late promoters (11, 27). Recently, *rIII* was suggested to play a role in the propagation of T4 in slow-growing host cells (28). Here, we present the preliminary results of *in vivo* and *in vitro* characterization of *rIII*. The results are analyzed in terms of a model that suggests direct molecular involvement of RIII in LIN as a new class of antiholin.

Materials and methods

Bacterial growth and induction

See **Table 1** for the full list of phages and bacteria strains used in this study. Bacterial strains were plated on standard LB-agar plate supplemented with the appropriate antibiotics (ampicillin, 100 μg mL^{-1}; chloramphenicol, 10 μg mL^{-1}; Kanamycin, 40 μg mL^{-1}). A single colony from a LB plate was used to inoculate 3 mL overnight culture at 30°C for λ lysogens and 37°C for non-lysogenic *E. coli* strains, as described before (21). Overnight cultures were diluted to A_{550} ~ 0.03 and grown at 30°C or 37°C with aeration. Bacterial growth and lysis were monitored as described (21) using a Gilford Stasar III sipping spectrophotometer (Gilford Instrument Inc, Oberlin, OH). The λ lysogens were induced as described (14, 21). All plasmid-cloned genes were induced with 1 mM isopropyl b-D-thiogalactosidase (IPTG).

Phage infection and preparation of phage lysates

Phage lysates were prepared by adding 10% $CHCl_3$ (v/v) to the *E. coli* cell culture after lysis , in either induced lysogens or by liquid culture infections, as described previously (19). The lysate was cleared by centrifugation at 5,000 x *g* and the

supernatant was filtered through a 0.22 μm syringe filter. Phage infection experiments were carried out as described (19, 21). For liquid culture infections, host *E. coli* cells were grown to A_{550} ~ 0.3 and infected at a multiplicity of infection (MOI) ~ 5. To observe plaque morphology, 100 μL overnight cultures of host cells were added to 3 mL of LB top agar and immediately poured on standard LB-agar plates. 5 μL of phage lysates with proper dilutions were spotted onto the top agar. For complementation experiment, BL21(DE3) *fhuA*::Tn*10* cells carrying pET11a vectors were grown to A_{550} ~ 1 at 37°C, and induced with 1mM IPTG for 2 h before mixed with LB top agar and poured onto LB plates containing proper antibiotics and 1mM IPTG. All plates were incubated ~16h at 37°C. The plaque sizes were analyzed using ImageJ software (NIH, Bethesda, MD).

Standard DNA manipulations and sequencing

All plasmids used in this study are listed in **Table 1**. Isolation of plasmid DNA, DNA amplification by polymerase chain reaction (PCR), DNA transformation, and DNA sequencing were performed as previously described (15, 22, 29). Oligonucleotides (primers) DNA sequences are listed in **Table 2**. All purified oligonucleotides (primers) were purchased from Integrated DNA technologies (Coralville, IA). Restriction and DNA-modifying enzymes were purchased from New England Biolabs (Ipswich, MA). Manufacturer's instructions were followed when performing reactions. The DNA sequence of all constructs was verified by sequencing service provided by Eton Bioscience (San Diego, CA).

PCR and plasmid construction

T4D phage lysate was directly used as the PCR template for cloning out T4 genes. Pfu DNA polymerase was used for all PCR reactions following standard

protocols provided by Promega (Madison, WI). Site-directed mutagenesis was performed as described (22). The *rIII* gene either with its native ribosome binding site (GAG) or a stronger ribosome binding site (AGGAG) was cloned into the medium-copy IPTG-inducible vector pZE12 (30). Plasmid pZE12-$RIII_o$ and pZE12-$RIII_s$ were constructed by inserting T4 DNA from nt 130738 to nt 131080 ($RIII_o$), or from nt 130785 to nt 131033 ($RIII_s$) into pZE12 between KpnI and XbaI sites. Plasmid pET11aRIII has the same insertion as pZE12$RIII_s$ between its NdeI and BamHI sites. Plasmid pZE12RI-RIII was made by inserting a tandem clone of *rI* and *rIII* genes with their original ribosome binding site into plasmid pZE12. These plasmids were transformed into a CQ21λ-t lysogen, in which the lambda holin gene *S* has been replaced by T4 gene *t* (14). In this system, RI or/and RIII can be expressed *in trans* to T from pZE12 plasmids by adding 1mM IPTG after lysogenic induction. A λS_{A52G} lysogen was used as a control, since the S_{A52G} confers a ~20 min lysis time, similar to the *t* gene (31). Plasmid pTB146 is a derivative of plasmid pET11a encoding an N-terminal his6-SUMO tag (29, 32). Plasmids encoding His-SUMO-tagged versions of RIII and nT (the N-terminal domain of T), pTB146-RIII and pTB146-nT were constructed by inserting codon 2-81 of the *rIII* gene, or codons 2-34 of the *t* gene (nt 160218 to nt 160322 of T4 genome), respectively, into the pTB146 plasmid between its SapI and XhoI sites.

Constructing T4 *rIII* deletion mutant

T4Δ*rIII* was constructed by homologous recombination between pZE12-Δ*rIII* and T4D, as described previously for T4Δ*rI* (19). pZE12- Δ*rIII* was made by deleting the *rIII* gene from plasmid pZE12-*rIII*-flank, which contains T4 DNA from nt 130231 to nt 131541 between its KpnI and XbaI sites, using our previously described method (33).

Plasmid pZE12- Δ*rIII* was transformed into *E.coli* strain MDS12 *tonA*::Tn*10* *lacI*^{q1}, and the transformants were grown to A_{550} ~ 0.4. The culture was infected with T4D phage at a MOI=10 for 3 h at 37°C with aeration, and then lysed by adding 10% v/v $CHCl_3$. T4 *rIII* recombinants in this lysate were enriched three times for early lysis as described (19). The enriched lysate was plated on *E. coli* B834 and screened for *r* plaque morphology. The Δ*rIII* deletion was confirmed by PCR and sequencing.

SDS-PAGE and Western blotting

SDS-PAGE and Western blotting were conducted as previously described (22) 10% trichloroacetic acid (TCA) was used to precipitate proteins from the whole-cell samples. Reducing sample loading buffer (SLB) supplemented with β-mercaptoethanol was used for resuspending protein samples unless otherwise indicated. RIII proteins transferred onto PVDF membrane were detected using rabbit polyclonal anti-RIII (α-RIII) antibody purchased from Genscript (Piscataway, NJ). The monoclonal anti-his-tag antibody (α-his) was purchased from Sigma-Aldrich (Carlsbad,CA). To detect proteins, blots were incubated overnight at 4°C with α-RIII or α-his at a dilution of 1:4000 in 3% milk-TBS buffer. Blots were developed with the West Femto SuperSignal Chemiluminescence kit purchased from Thermo Fisher Scientific (Rockford, IL). The chemiluminescence signal was detected using a Bio-Rad Chemidoc XRS (Bio-Rad Laboratories, Hercules, CA). Images were obtained and analyzed by Quantity One 1-D Analysis Software (Bio-Rad Laboratories, Philadelphia, PA).

206 **Bacterial two hybrid assay**

207 Bacterial two hybrid (B2H) assays were conducted as described previously (34-
208 36). Plasmids were constructed by inserting codons 2-81 of the *rIII* gene, or codons 2-
209 34 of the *t* gene into plasmids pCH363, pKNT25, pCH364, and pKT25, as described
210 (36). Different pairs of plasmid were transformed into strain DHP1 and grown to A_{550} ~
211 0.3 in LB with 0.2% glucose and appropriate antibiotics (ampicillin, 50 μg mL^{-1};
212 kanamycin, 25 μg mL^{-1}). For the plate assay, 5 μL of cell cultures were spotted on M9
213 minimal media plates supplemented with 0.2% glucose, 40 μg mL^{-1} X-Gal, 150 μM
214 IPTG and proper antibiotics and incubated for 48h at 25°C.

215 **Pull-down assays**

216 Plasmid pET11a and pTB146 derivatives described above were transformed into
217 BL21(DE3) *fhuA*::Tn*10* strains. Pull-down assays were conducted as instructed by
218 manufacturer protocol from Dynabeads® His-Tag Isolation and Pulldown kit (Thermo
219 Fisher Scientific, Rockford, IL). All incubation and reaction were carried out in 4°C and
220 beads were collected using DynaMag™-2 Magnet (Thermo Fisher Scientific). All
221 samples were resuspended in SLB and boiled for 5 min to elute proteins, which were
222 then analyzed by SDS-PAGE and Western blotting, which were performed as described
223 above.
224

225 **Results**

226 ***rIII* is required for LIN in both *E. coli* B and K-12 background**

227 The role of *rIII* in LIN has been ambiguous, with reports differing in whether *rIII*
228 was required on *E. coli* B but not K-12 strains (6, 9, 37). In our hands, the classic *rIII*
229 alleleT4*r67*, which was used as the standard allele in the early T4 genetic map studies,
230 formed r-type plaques on the lawns of both *E. coli* B834 and MG1655 (**Fig. 2A**), with
231 somewhat smaller plaques compared to those formed by T4*rI*, but significantly larger
232 than wt T4 plaques (**Table 3**). It was also reported that different T4 *rIII* mutants differed
233 in plaque size, suggesting a possible correlation between the location of mutations on
234 *rIII* locus and plaque morphology (38). However, when we compared plaque
235 morphologies of four different T4 *rIII* defective mutants (T4*r67*, T4*rBB9*, T4*rES35*, and
236 T4rES40) on B834, we did not observe significant differences (**Table 3**). Nevertheless,
237 as the first step for interrogating the role of *rIII* in LIN, we constructed an *rIII* deletion
238 allele, T4Δ*rIII*, to eliminate the potential for partial reversion. As shown in **Table 3** and
239 **Fig. 2A**, T4Δ*rIII* formed r-type plaques that were larger than wt plaques, but smaller
240 than those of T4*rI*. Moreover, the wt plaque morphology could be complemented by a
241 plasmid-borne *rIII* gene (**Fig. 2B**). In infections of both *E. coli* Bor K-12 cultures under
242 conditions where the wt T4 exhibited LIN, T4Δ*rIII* infections showed lysis at ~25 min, in
243 both cases reproducibly later than the lysis time of T4Δ*rI* (~18 min), (**Fig. 3A**). The
244 simplest notion, based on the established role of RI in LIN, is that RI expressed in the
245 T4Δ*rIII* infection causes transient LIN, and that, by extension, RIII is required for stable
246 LIN in both *E. coli* B and K-12 strains.
247

248 **Identification of the RIII protein**

249 *rIII* encodes an 82aa polypeptide without any secretion signals (Fig. 4A) and had
250 not been identified as a protein species in T4-infected cultures. We raised a polyclonal
251 antibody against an RIII oligopeptide sequence predicted to be highly immunogenic
252 (**Fig. 4A**). The RIII protein could be visualized by immunoblotting in samples taken from
253 cells infected with T4wt, but not with T4Δ*rIII* (**Fig. 4B**); the mobility of this RIII species
254 corresponded to a slightly lower molecular mass than predicted (8.9 kDa versus 9.3 kDa
255 predicted), presumably due to the high content of charged residues (24 out of 82) (**Fig.**
256 **4A**).

257 **Recapitulating the role of RIII in LIN in the λ context**

258 To address the role of RIII in LIN, we used a convenient system based on the
259 inducible lambda prophage, λ-t, in which the λ holin gene *S* is replaced by T4 *t* (14). Not
260 only was this hybrid phage previously shown to recapitulate T4 lysis timing and LIN at
261 physiological levels of expression, it allows the co-expression of selected T4 genes
262 cloned in inducible plasmid vectors without the confounding effects of T4-mediated host
263 DNA degradation and translational repression(14, 15, 21, 39). This system mimics the
264 T-dependent lysis in the λ context where effects of T4 genes other than *t* are excluded.
265 To provide RIII in trans, the *rIII* gene was cloned into a medium copy-number plasmid
266 vector pZE12 (30). Two isogenic clones were constructed with different Shine-Dalgarno
267 (SD) sequences serving the *rIII* cistron, one the relatively weak native sequence (GAG)
268 and the other with a stronger near-consensus sequence (AGGAG). The resulting
269 plasmids pZE12RIII$_o$ (original SD sequence) and pZE12RIII$_s$ (strong SD sequence)
270 were transformed into the λ-t lysogen. Induction of the λ-t lysogen resulted in

reproducible and sharply defined lysis at ~ 20 min; induction of pZE12RIII$_s$ with IPTG conferred a mild but reproducible lysis delay of ~5 min (**Fig. 3B**). In contrast, lysis was much more severely affected by induction of an isogenic clone of the T4 antiholin gene *rI*, as previously shown (21). Induction of pZE12RIII$_o$ did not affect the lysis timing, probably due to the lower protein expression level (Data not shown).

We next asked if RIII can extend RI-mediated LIN. An isogenic plasmid with *rI* and *rIII* cloned in tandem was constructed and introduced into the λ-t lysogen. Induction of this plasmid, pZE12RI-RIII, led to a drastically delayed LIN compared to induction of either pZE12RIII$_s$ or pZE12RI (**Fig. 3B**); under these conditions, the LIN state lasted up to 80 min and then gradually deteriorated. Using this system, we tested three *rIII* missense alleles isolated by UV mutagenesis: G24D, H42R, and A70V (9) (**Fig. 4A**). In the absence of RI, two of the alleles, G24D and H42R, exhibited a slight but reproducible LIN defect, although the phenotype was subtle due to the relatively small effect of the parental *rIII* allele under these conditions (**Fig. 3C**). Co-induction of these *rIII* with *rI*, however, resulted in distinct intermediate LIN defects, with lysis times ranging from 40 min~60 min, indicating these are partially defective alleles, at least in the lambda context (**Fig. 3C**). The lysis blockage was *t*-specific, as indicated by the fact that isogenic experiments with a lambda holin allele, S_{A52G}, which has an early lysis phenotype that matches the normal *t* lysis time (31), did not show lysis delays in inductions of pZE12RIII$_s$, pZE12RI or pZE12RI-RIII (**Fig. 3B**). Taken together, these data indicated that RIII has T-specific antiholin activity.

RIII binds to the cytoplasmic N-terminus of T

Next we addressed the molecular basis of RIII participation in LIN. The simplest hypothesis is, like other antiholins, including RI, RIII affects holin triggering by directly binding to holin T and blocking hole formation in the IM. Since RIII has no membrane or export signals (**Fig. 4A**), the only possible target for RIII is the N-terminal cytoplasmic domain of T (nT), which has 34aa, and is required for holin function (15). To test this idea, we used the bacterial two hybrid system, based on intragenic complementation of CyaA function (34). We fused the nT, wt RIII, and four RIII mutant allele sequences to various combinations of the T25 and T18 fragments of CyaA. As shown in **Fig. 5A**, this system revealed a strong self-interaction of RIII *in vivo*, which was abolished in the G24D allele, partially affected by H42R, and unaffected by L43Q or R75C. The transformants carrying plasmids expressing T18-RIII and T25-nT resulted in light but reproducible signals (**Fig. 5B**), suggesting a relatively weak interaction between RIII and nT. Significantly, none of the four RIII mutant fusions retained the nT-binding ability (**Fig. 5B).** These results correlate with the liquid culture lysis results (**Fig. 3C**) and indicate the nT-RIII interaction is affected by the changes in the lysis-defective RIII alleles.

To address the nT-RIII interaction in vitro, we constructed versions of nT and RIII tagged at the N-terminus with the His6-Sumo moiety (See Materials and Methods). After induction in a T7-based over-expression system, both His6-Sumo-nT and His6-Sumo-RIII accumulated as soluble forms (**Fig. 6, top panel, lanes 2-5**). To detect complexes formed *in vitro*, the SUMO-tagged nT and RIII proteins were bound to magnetic beads, mixed with cell lysates containing wt RIII or mutant $RIII_{H42R}$ protein, fractionated as

bound and unbound, and then analyzed by immunoblotting. The results showed that both wt RIII and mutant $RIII_{H42R}$ proteins form complexes with His6-Sumo-RIII, but only wt RIII complexes with His6-Sumo-nT (**Fig. 6, bottom panel**). The simplest interpretation is that the H42R mutation completely abrogates the RIII-nT interface but not the RIII homo-oligomerization interface, which is consistent with the results of the bacterial two-hybrid experiments.

The cytoplasmic N-terminal domain of T can block lysis inhibition in an RIII-specific manner

The finding that RIII binds nT in vitro and in *E. coli* in the context of the two-hybrids suggested that the *r* phenotype could be imposed in vivo by titrating the RIII produced in a T4 infection with the Sumo-tagged nT derivative. To test this idea, we plated T4 on lawns of cells induced for the over-expression of His6-Sumo-nT; under these conditions, T4 wt generated plaques distinctly larger and cleared compared to those generated on the isogenic control strain expressing the His6-Sumo tag (**Fig. 7**). Neither T4*rIII* nor T4Δ*rIII* plaque morphology was affected by overexpression of nT (**Fig 7**).

Discussion

Among the Caudovirales, the lysis timing effected by the holin defines the length and fecundity of the phage infection cycle. Mutational analysis has shown that holin-mediated lysis timing can be drastically altered by single missense changes (15, 39-41), leading to the suggestion that this extreme mutational sensitivity is an evolutionary fitness factor, allowing phages to mutate rapidly to a radically different length of life

337 cycle in response to altered environmental conditions (42). Despite the implied
338 correlation between lysis timing and the environment, the T4 LIN phenomenon remains
339 the only documented example of real-time regulation of lysis timing. Genetic analysis
340 has shown that mutations in two of the classic T4 plaque-morphology loci, *rI* and *rV*, the
341 latter allelic to the *t* holin gene, confer an absolute defect in LIN. Our work had shown
342 that RI is a secreted protein that is initially synthesized as periplasmic protein tethered
343 to the membrane with an N-terminal signal-anchor-release (SAR) domain (19). The
344 presence of the SAR domain allows it to release into the periplasm and also confers
345 extreme proteolytic instability on RI. Over-expression of the wt *rI* gene was shown to
346 impose a delay on T-holin triggering in the lambda context. A chimeric *rI* gene in which
347 the SAR domain was replaced by a cleavable signal sequence generated a
348 proteolytically stable periplasmic RI and, expressed in trans to *t*, imposed a stable LIN
349 state. A model has been proposed in which an unknown LIN signal is generated by a
350 super-infecting T4 virion. Under these conditions, it is suggested that the T4 Spackle
351 and Imm proteins force the superinfecting virion to eject its capsid contents ectopically
352 into the host periplasm (43). Some component of these virion contents, which include
353 both the T4 genomic DNA and ~1000 protein molecules (11, 37), acts as a signal to
354 stabilize the periplasmic RI protein. In this model, RI accumulates and binds to the
355 periplasmic domain of the T4 holin T in a manner that T triggering is inhibited.(19).
356 Significant progress has been made on the RI-T interaction. The soluble domain of RI,
357 sRI, has been purified and shown to be largely alpha-helical in structure (22). In
358 addition, the sRI molecule was able to bind the soluble domain of T, sT (22, 44), and
359 prevent it from aggregation. Crystal structures of sRI and the sRI:sT complex have been

360 determined (44). However, major gaps remained in our understanding of the LIN
361 phenomenon. First of all, the signal provided by the superinfecting phage is completely
362 unknown. In addition, the possible role of other *r* loci, most notably *rIII*, was not reflected
363 in the model.

364 In this study we have shown that *rIII* is also unambiguously required for LIN on
365 both *E. coli* K-12 and B hosts, resolving a long-standing controversy (9, 11). Moreover,
366 we have shown the *rIII* gene expressed *in trans* to the T4 holin gene *t* can effect a small
367 but reproducible lysis delay in a T-specific manner. In addition, expression of *rIII*
368 significantly stabilized the LIN state imposed by over-expression of wt *rI*, which
369 otherwise imposes a lysis delay that collapses after ~45 min. Since RIII is a cytoplasmic
370 protein, the simplest notion is that RIII acts by binding to the short cytoplasmic domain
371 of T, nT. Evidence supporting this was obtained from bacterial two-hybrid analysis and
372 pull-down assays, which revealed a specific interaction between nT and the full-length
373 RIII polypeptide. Importantly, known dysfunctional *rIII* missense mutations caused a
374 defect in the RIII-mediated stabilization of RI-LIN. Finally, bacterial two-hybrid evidence
375 was provided showing that RIII has dimerizing or oligomerizing propensity, which may
376 be functionally important in view of the fact that one of the known *rIII* defective missense
377 mutations abrogates the response.

378 Taken together, these results indicate that both RI and RIII are, strictly defined,
379 specific antiholins of the T4 holin T, and suggest an expansion of our previous model to
380 include inhibitory interactions on both sides of the cytoplasmic membrane (**Fig. 8**). In
381 this scenario, RI acts as the LIN master regulator by receiving the signal generated by
382 the super-infecting virion. Stabilization of RI leads to the formation of RI-T complexes

that prevent the T protein from participating in the holin triggering pathway. The available evidence indicates that holin triggering occurs when the holin reaches a critical two-dimensional concentration and forms large oligomers, or rafts, within which the lethal holes are formed (42, 45). The simplest notion is that RI may simply block homo-oligomerization of T and thus T-triggering, which is consistent with the ability of sRI to prevent aggregation of sT (20). In our new model, we suggest that RIII participates in LIN by stabilizing the RI-T complexes. Indeed, the sRI:sT crystal structures were in the form of sT:sRI:sRI:sT hetero-tetramers (44). Thus an attractive notion is that in the onset of LIN, T-RI-RI-T heterotetramers are formed providing a symmetric binding site for RIII dimers to bind to the cytoplasmic nT domains (**Fig. 8**). It should be noted that, in this perspective, RIII is the first example of an antiholin with no secretory or membrane signal, and also that the RI-RIII combination is the first example of a multiple-antiholin system. Since stabilizing RI by removal of the SAR domain can lead to stable LIN without the participation of RIII, we propose to designate RI as the antiholin with RIII as a co-antiholin.

As noted above, major gaps remain in our understanding of the T4 LIN phenomenon, which deserves attention not only because of its historical status, but as a richly-documented phenomenon that may be important in our understanding of phage propagation in liquid culture and in environmental scenarios that may be relevant to phage-based therapeutics. Immediate future efforts will be directed at determining the nature of the RIII-nT interaction at the structural level.

Acknowledgement

This research was supported by Public Health Service grant GM27099 to R.Y. and by funding from the Center for Phage Technology (CPT). The CPT is jointly supported by Texas A&M University and Texas A&M AgriLife Research. We thank Yi Duan and Allyssa Miller from the Herman laboratory for providing plasmids, strains, and advice for implementation of the bacterial two-hybrid assay. We also thank the Young laboratory and Center for Phage Technology members, past and present, for their helpful discussion, criticisms and suggestions.

Literature cited or References:

1. **Hershey AD.** 1946. Mutation of Bacteriophage with Respect to Type of Plaque. Genetics **31:**620-640.
2. **Doermann AH.** 1948. Lysis and Lysis Inhibition with Escherichia coli Bacteriophage. J Bacteriol **55:**257-276.
3. **Hershey AD, Chase M.** 1951. Genetic recombination and heterozygosis in bacteriophage. Cold Spring Harb Symp Quant Biol **16:**471-479.
4. **Benzer S.** 1955. Fine Structure of a Genetic Region in Bacteriophage. Proc Natl Acad Sci U S A **41:**344-354.
5. **Crick FH, Barnett L, Brenner S, Watts-Tobin RJ.** 1961. General nature of the genetic code for proteins. Nature **192:**1227-1232.
6. **Benzer S.** 1957. The Elementary Units of Heredity. *In* WILLIAM D. McELROY BG (ed.), The Chemical Basis of Heredity. Johns Hopkins University Press, Baltimore.
7. **Hershey AD, Rotman R.** 1948. Linkage Among Genes Controlling Inhibition of Lysis in a Bacterial Virus. Proc Natl Acad Sci U S A **34:**89-96.
8. **Hershey AD.** 1946. Spontaneous mutations in bacterial viruses, Cold Spring Harb Symp Quant Biol, vol. 11: 67-77. Cold Spring Harbor Laboratory Press.
9. **Burch LH, Zhang L, Chao FG, Xu H, Drake JW.** 2011. The bacteriophage T4 rapid-lysis genes and their mutational proclivities. J Bacteriol **193:**3537-3545.
10. **Krylov VN, Yankovsky NK.** 1975. Mutations in the new gene stIII of bacteriophage T4B suppressing the lysis defect of gene stII and a gene e mutant. J Virol **15:**22-26.
11. **Paddison P, Abedon ST, Dressman HK, Gailbreath K, Tracy J, Mosser E, Neitzel J, Guttman B, Kutter E.** 1998. The roles of the bacteriophage T4 r genes in lysis inhibition and fine-structure genetics: a new perspective. Genetics **148:**1539-1550.
12. **Dressman HK, Drake JW.** 1999. Lysis and lysis inhibition in bacteriophage T4: rV mutations reside in the holin t gene. J Bacteriol **181:**4391-4396.
13. **Young R.** 1992. Bacteriophage lysis: mechanism and regulation. Microbiol Rev **56:**430-481.
14. **Ramanculov E, Young R.** 2001. Functional analysis of the phage T4 holin in a lambda context. Mol Genet Genomics **265:**345-353.
15. **Moussa SH, Lawler JL, Young R.** 2014. Genetic dissection of T4 lysis. J Bacteriol **196:**2201-2209.
16. **Josslin R.** 1970. The lysis mechanism of phage T4: mutants affecting lysis. Virology **40:**719-726.
17. **Summer EJ, Berry J, Tran TA, Niu L, Struck DK, Young R.** 2007. Rz/Rz1 lysis gene equivalents in phages of Gram-negative hosts. J Mol Biol **373:**1098-1112.
18. **Bode W.** 1967. Lysis inhibition in Escherichia coli infected with bacteriophage T4. J Virol **1:**948-955.
19. **Tran TA, Struck DK, Young R.** 2007. The T4 RI antiholin has an N-terminal signal anchor release domain that targets it for degradation by DegP. J Bacteriol **189:**7618-7625.

20. **Tran TA, Struck DK, Young R.** 2005. Periplasmic domains define holin-antiholin interactions in t4 lysis inhibition. J Bacteriol **187:**6631-6640.
21. **Ramanculov E, Young R.** 2001. An ancient player unmasked: T4 rI encodes a t-specific antiholin. Mol Microbiol **41:**575-583.
22. **Moussa SH, Kuznetsov V, Tran TA, Sacchettini JC, Young R.** 2012. Protein determinants of phage T4 lysis inhibition. Protein Sci **21:**571-582.
23. **Blasi U, Chang CY, Zagotta MT, Nam KB, Young R.** 1990. The lethal lambda S gene encodes its own inhibitor. EMBO J **9:**981-989.
24. **White R, Tran TA, Dankenbring CA, Deaton J, Young R.** 2010. The N-terminal transmembrane domain of lambda S is required for holin but not antiholin function. J Bacteriol **192:**725-733.
25. **To KH, Dewey J, Weaver J, Park T, Young R.** 2013. Functional analysis of a class I holin, P2 Y. J Bacteriol **195:**1346-1355.
26. **Barenboim M, Chang CY, dib Hajj F, Young R.** 1999. Characterization of the dual start motif of a class II holin gene. Mol Microbiol **32:**715-727.
27. **Luke K, Radek A, Liu X, Campbell J, Uzan M, Haselkorn R, Kogan Y.** 2002. Microarray analysis of gene expression during bacteriophage T4 infection. Virology **299:**182-191.
28. **Golec P, Karczewska-Golec J, Voigt B, Albrecht D, Schweder T, Hecker M, Wegrzyn G, Los M.** 2013. Proteomic profiles and kinetics of development of bacteriophage T4 and its rI and rIII mutants in slowly growing Escherichia coli. J Gen Virol **94:**896-905.
29. **Berry J, Savva C, Holzenburg A, Young R.** 2010. The lambda spanin components Rz and Rz1 undergo tertiary and quaternary rearrangements upon complex formation. Protein Sci **19:**1967-1977.
30. **Lutz R, Bujard H.** 1997. Independent and tight regulation of transcriptional units in Escherichia coli via the LacR/O, the TetR/O and AraC/I1-I2 regulatory elements. Nucleic Acids Res **25:**1203-1210.
31. **Johnson-Boaz R, Chang CY, Young R.** 1994. A dominant mutation in the bacteriophage lambda S gene causes premature lysis and an absolute defective plating phenotype. Mol Microbiol **13:**495-504.
32. **Bendezu FO, Hale CA, Bernhardt TG, de Boer PA.** 2009. RodZ (YfgA) is required for proper assembly of the MreB actin cytoskeleton and cell shape in E. coli. EMBO J **28:**193-204.
33. **Hansson MD, Rzeznicka K, Rosenback M, Hansson M, Sirijovski N.** 2008. PCR-mediated deletion of plasmid DNA. Anal Biochem **375:**373-375.
34. **Karimova G, Pidoux J, Ullmann A, Ladant D.** 1998. A bacterial two-hybrid system based on a reconstituted signal transduction pathway. Proc Natl Acad Sci U S A **95:**5752-5756.
35. **Battesti A, Bouveret E.** 2012. The bacterial two-hybrid system based on adenylate cyclase reconstitution in Escherichia coli. Methods **58:**325-334.
36. **Miller AK, Brown EE, Mercado BT, Herman JK.** 2016. A DNA-binding protein defines the precise region of chromosome capture during Bacillus sporulation. Mol Microbiol **99:**111-122.
37. **Christopher K. Mathews EMK, Gisela Mosig, Peter B. Berget.** 1983. Bacteriophage T4. American Society of Microbiology, Wachington, D.C.

Journal of Bacteriology

38. **Raudonikiene A, Nivinskas R.** 1992. Gene rIII is the nearest downstream neighbour of bacteriophage T4 gene 31. Gene **114:**85-90.
39. **Ramanculov E, Young R.** 2001. Genetic analysis of the T4 holin: timing and topology. Gene **265:**25-36.
40. **Pang T, Park T, Young R.** 2010. Mutational analysis of the S21 pinholin. Mol Microbiol **76:**68-77.
41. **Raab R, Neal G, Garrett J, Grimaila R, Fusselman R, Young R.** 1986. Mutational analysis of bacteriophage lambda lysis gene S. J Bacteriol **167:**1035-1042.
42. **Young R.** 2013. Phage lysis: do we have the hole story yet? Curr Opin Microbiol **16:**790-797.
43. **Obringer JW.** 1988. The functions of the phage T4 immunity and spackle genes in genetic exclusion. Genet Res **52:**81-90.
44. **Kuznetsov VB.** 2011. Structural Studies of Phage Lysis Proteins and Their Targets. Doctoral dissertation, Texas A&M University, College Station.
45. **To KH, Young R.** 2014. Probing the structure of the S105 hole. J Bacteriol **196:**3683-3689.

552 **Figure Legends**

553 **FIG 1** Topology of T4 holin T -antiholin RI interaction. T is an inner membrane protein
554 with a single TMD (shown as a solid cylinder) and an amphipathic helix (shown as a
555 white cylinder). RI has a SAR (Signal Anchor-Release) domain (shown as a dash line
556 rectangle) which allows RI to be spontaneously released in to the periplasm (19). If
557 stabilized by the LIN signal, periplasmic RI binds to the C-terminal globular periplasmic
558 domain of T. IM, inner membrane.

559 **FIG 2** Plaque morphologies of T4 and its *r* mutants. **(A)** Plaque morphology of T4 wt
560 (T4D) and T4 mutants on either *E. coli* B strain (B834) or *E. coli* K-12 strain (MG1655).
561 The black bar represents 2.5mm. Average plaque sizes of T4D, T4Δ*rIII,* T4*rIII* and T4Δ*rI*
562 on *E. coli* B834 or *E. coli* MG1655 are listed in Table 3. **(B and C)** Complementation of
563 *r* plaque morphology. T4 *rIII* mutants plated on *E. coli* strains expressing wt RIII restored
564 wt T4 plaque morphology, whereas the expression of RIIIH42R did not. In B, differences
565 in plaque sizes were shown as the ratio of the average phage plaque radius (r) to the
566 average plaque radius of T4D plated on B834 (r_0). 1, MG1655; 2, BL21(DE3)
567 *fhuA*::Tn*10* no plasmid; 3, BL21(DE3) *fhuA*::Tn*10* pET11a pET11a-RIII; 4, BL21(DE3)
568 *fhuA*::Tn*10* pET11a-$RIII_{H42R}$.

569 **FIG 3 (A)** Lysis in infections of T4 and derivatives infecting *E. coli* B strain B834 (Left,
570 solid line) or K-12 strain MG1655 (right, dotted line). ×, no phage; ●, T4D (wt); ▲,
571 T4Δ*rI*; △, T4Δ*rIII*. Cultures were grown to A_{550} ~ 0.25 at 37°C, then infected with T4 at
572 MOI~5. **(B)** Inductions (at t=0) of CQ21*λ*-t (Left, solid symbols) or CQ21*λ*S_{A52G} (right,
573 open symbols) lysogens carrying indicated genes cloned under IPTG control in the

574 context of the pZE12 plasmid. Plasmids were also induced by addition of 1mM IPTG at
575 t=0. ×, luc (negative control); ▲ and △, RI; ● and ○, RIIIs; ◆ and ◇, RI-RIII. **(C)** RIII
576 missense mutants exhibit intermediate LIN phenotype. CQ21*λ*-t lysogens carrying
577 pZE12 plasmids with indicated genes were induced at t=0. ×, luc; ▲, RI; ●, RIIIs; ◆,
578 RI-RIII. Left pane with dotted lines: □, $RIII_{G24D}$; ◇, $RIII_{H42R}$; ▽, $RIII_{A70V}$. Right panel with
579 solid lines: □, RI-$RIII_{G24D}$; ◇, RI-$RIII_{H42R}$; ▽, RI-$RIII_{A70V}$.

580 **FIG 4 (A)** Primary structure of RIII and N-terminus of T4 holin T (nT) with LIN-defective
581 and lysis-defective alleles indicated by black arrows. Conserved residues are
582 underlined. The shaded area represents the oligopeptide used to raise the anti-RIII
583 antibody. Predicted secondary structure is indicated: white box, helix; solid line, turn;
584 white arrow, beta-sheet; grey box, amphipathic helix. **(B)** RIII protein accumulates
585 during infection. For each sample, 1 A600 equivalent of cells was loaded. The anti-RIII
586 antibody was used in Western blotting. Black arrow indicates predicted molecular mass
587 (9.3kDa) for RIII monomer.

588 **FIG 5** Bacterial two-hybrid results showing self-interaction of RIII **(A)** and interaction of
589 RIII and N-terminus of T (nT) **(B)**. T18, protein fused to T18 fragment of CyaA protein;
590 T25, protein fused to T25 fragment of CyaA. Negative control (--) indicates T18 or T25
591 fragments without RIII or nT fusion.

592 **FIG 6** I*n vitro* interaction between nT and RIII. His-Sumo-tagged nT or RIII was bound
593 to anti-his Dynabeads, and RIII protein pulled down by Dynabeads was analyzed by
594 Western blotting. His-sumo tag only (lane 1, dash black arrow), His-sumo nT (lane 2

and 4, black arrow head), His-sumo RIII (lane 3 and 5, white arrow) are shown in the upper panel as the result of western blotting using anti-his antibody. RIII protein (solid black arrow) is visualized in the bottom panel using anti-RIII antibody.

FIG 7 Rescue of *r* plaque morphology by overexpression of the N-terminus of T (nT). **(A)** T4 phages were plated on lawns of *E. coli* BL21(DE3) *fhuA*::Tn*10* carrying control plasmid expressing His-sumo-nT (pTB146-nT, bottom panels) or His-sumo (pTB146, top panels, neg control). Black bar represents 2.5mm. **(B)** Quantification of plaque sizes were shown as the ratio of the average plaque radius (r) to the ratio of T4D plaques plated on pTB146 (r_0). Black bar, T4D; Patterned bar, T4Δ*rIII*; White bar, T4r*III*.

FIG 8 The current model of LIN involving two antiholins. Both RI and RIII are required for the stable LIN. **(A)** In a single phage infection, antiholin RI will be degraded by periplasmic protease DegP after spontaneous release into the periplasm. Cell lysis occurs at ~ 25 min. **(B)** In a superinfection, the DNA of a superinfecting T4 phage will be ectopically ejected into the periplasm, generating the “signal” to stabilize the periplasmic antiholin RI. This leads to accumulation of RI, which then binds the periplasmic domain of T, in a T-RI-RI-T heterotetramer. This facilitates the binding of cytoplasmic antiholin RIII to the N-terminus of T. This unique, sandwich-like structure spanning two cell compartments robustly blocks participation of T in hole-formation.

616 **TABLE 1** Phages, strains, and plasmids used in this study.

Phages	**Description**	**Source**
T4wt	Bacteriophage T4D	Laboratory Stock
T4*rIII*	T4*r67*. H42 to R (CAU to CGU) mutation in *rIII* locus.	Laboratory Stock
T4Δ*rI*	Complete deletion of *rI* from nt 59204 to nt 59496 in T4D genome	(19)
T4Δ*rIII*	Complete deletion of *rIII* from nt 130779 to nt 131042 in T4D genome	This study
λ-t	λwith holin gene *S* replaced with T4 holin gene *t*	(14)
λS_{A52G}	λcI857 carrying Ala52Gly early lysis allele of *S* holin gene.	(31)
T4rBB9	W16 to stop (UGG to UGA) mutation in *rIII* locus	Laboratory Stock
T4rES35	H42 to Q (CAU to CAA) mutation in *rIII* locus	Laboratory Stock
T4rES40	K82 to E (AAG to GAG) mutation in *rIII* locus	Laboratory Stock
Bacteria Strains	**Description**	**Source**
CQ21	*E. coli* K-12 *ara leu lacI^q purE gal his argG rpsL xul mtl ilv*	Laboratory Stock
CQ21 λ-t	CQ21 lysogen carrying λ-t prophage	(14)
CQ21 λS_{A52G}	CQ21 lysogen carrying λSA52G prophage	This study
BL21(DE3) *fhuA*::Tn*10*	*E. coli* B *ompT* r_B^- m_B^- (*P_{lac}UV5::*T7 *gene1*) *slyD::Kan fhuA*::Tn*10*	Laboratory Stock
B834	*E. coli* B *ompT* r_B^- m_B^- *met*$^-$	Laboratory Stock
MG1655	*E. coli* F- *lambda- ilvG- rfb-50 rph-1*	Laboratory Stock
MDS12 *tonA*::Tn*10* *lacI*^{q1}	MG1655 with 12 deletions, totaling 376,180 nt including cryptic prophages	(19)
DHP1	*E. coli* F- *cya-99 araD139 galE15, galK16, rpsL1 (Strr) hsdR2 mcrA1 mcrB1*	(36)
Plasmids	**Description**	**Source**
pZE12	ColE1 origin; $P_{LlacO-1}$ (PL promoter with three lacO	(30)

	operators); AmpR	
pZE12-luc	Luciferase gene luc cloned under $P_{LlacO-1}$	(30)
pZE12RI	T4 *rI* cloned under $P_{LlacO-1}$ with native SD	(21)
pZE12RIII$_o$	T4 *rIII* cloned under $P_{LlacO-1}$ with native SD	(21)
pZE12RIII$_s$	T4 *rIII* cloned under $P_{LlacO-1}$ with plasmid SD	This study
pZE12RI-RIII	Tandem clone of *rI- rIII* inserted between KpnI and XbaI site	This study
pET11a-RIII	pBR322 origin, T7 promoter, carrying codon 1-82 of *rIII*	This study
pET11a-RIII$_{H42R}$	H42 to R (CAU to CGU) mutation in *rIII*	This study
pTB146	*bla lacI*^{q} PT7::h-sumo	(32)
pTB146-RIII	Codon 2-82 of *rIII* gene inserted between SapI and XhoI site	This study
pTB146-nT	Codon 2-34 of *t* gene inserted between SapI and XhoI site	This study
pCH364	T18-empty (AmpR);N-terminal tag	(36)
pKNT25	Empty-T25 (KanR); C-terminal tag	(35, 36)
pKT25	T25-empty (KanR); N-terminal tag	(35, 36)
pCH364RIII	Codon 2-82 of *rIII* gene inserted between BamHI and EcoRI site	This study
pKNT25RIII	Codon 2-82 of *rIII* gene inserted between XbaI and EcoRI site	This study
pKT25nT	Codon 2-34 of *t* gene inserted between BamHI and EcoRI site	This study

TABLE 2 List of oligonucleotides (primers)

Primer name	Sequence	Source
$RIII_S$ CLONING F	CGGTACATTAAACAATTACAACACGCTC	This study
$RIII_S$ CLONING R	GGCTCTAGATTACTTCAGTGTTACCACAAAGTG	This study
$RIII_S$ PET F	GGAATTCCATATGATTAAACAATTACAACACGCTC	This study
$RIII_S$ PET R	GCGGGATCCTTACTTCAGTGTTACCACAAAGTG	This study
RIII DEL +500 F	GGGGTACCCATCTGTTAACAAAAAGGAAAAACG	This study
RIII DEL -500 R	GCTCTAGAGCGTTCAGATTAATCGTTTTCA	This study
RIII DEL MIX F	TTTTAATCTCTAACGAGGGAGATTCACTGCCT TAGTGTGAGC	This study
RIII DEL MIX R	CCGAGTTTTAATCTCTAACGAGGGAGATTCAC TGCCTTAGT	This study

TABLE 3 Mean diameter of phage plaques (mm)

Host / Phage	B834	MG1655	BL21 (DE3)	BL21 (DE3) pET11aRIII	BL21 (DE3) pET11a RIII-H42R	BL21 (DE3) pTB146	BL21 (DE3) pTB146-nT
T4D	0.57 (±0.04)	0.67 (±0.04)	0.63 (±0.06)	0.53 (±0.05)	0.57 (±0.05)	0.68 (±0.04)	1.07 (±0.05)
T4*rIII*	1.09 (±0.09)	1.43 (±0.07)	1.07 (±0.09)	0.62 (±0.03)	0.92 (±0.08)	1.32 (±0.08)	1.38 (±0.06)
T4Δ*rIII*	0.92 (±0.08)	1.12 (±0.06)	0.95 (±0.07)	0.52 (±0.06)	0.86 (±0.08)	1.13 (±0.08)	1.17 (±0.07)
T4Δ*rI*	1.29 (±0.09)	1.88 (±0.11)	1.24 (±0.07)	1.21 (±0.03)	1.34 (±0.06)	-	-
T4rBB9	0.89 (±0.15)	-	-	-	-	-	-
T4rES35	1.02 (±0.05)	-	-	-	-	-	-
T4rES40	1.05 (±0.05)	-	-	-	-	-	-

617

Figure 1

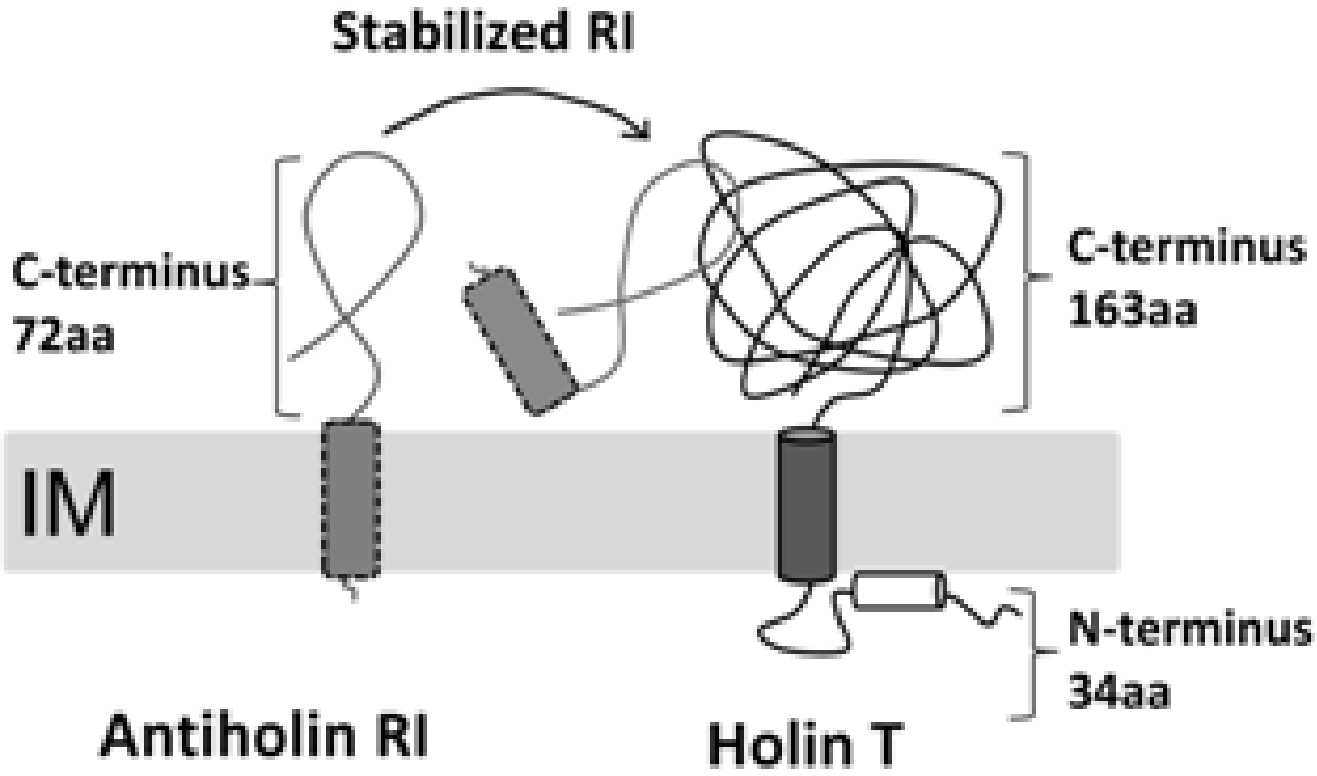

Figure 2

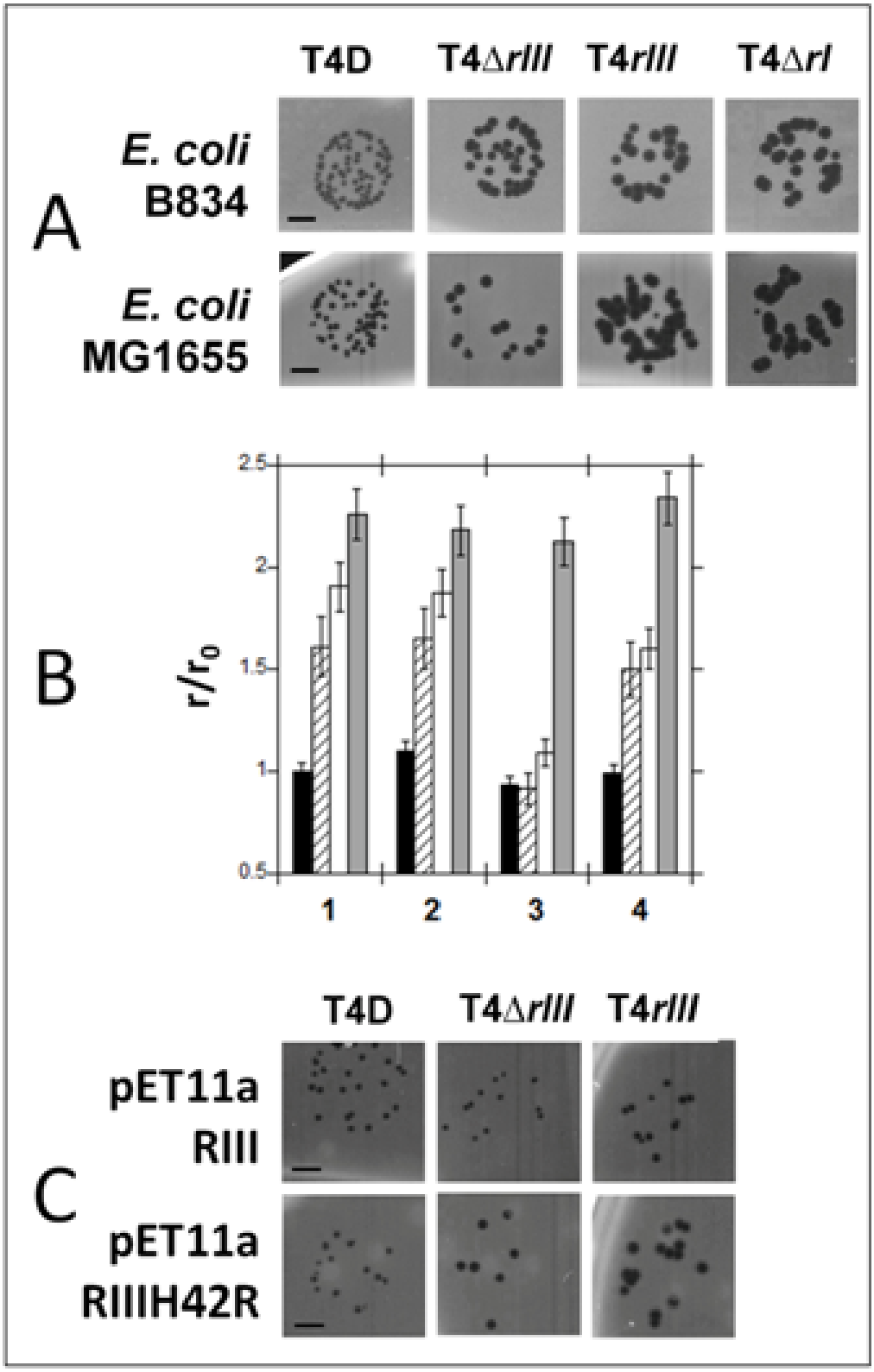

Figure 3

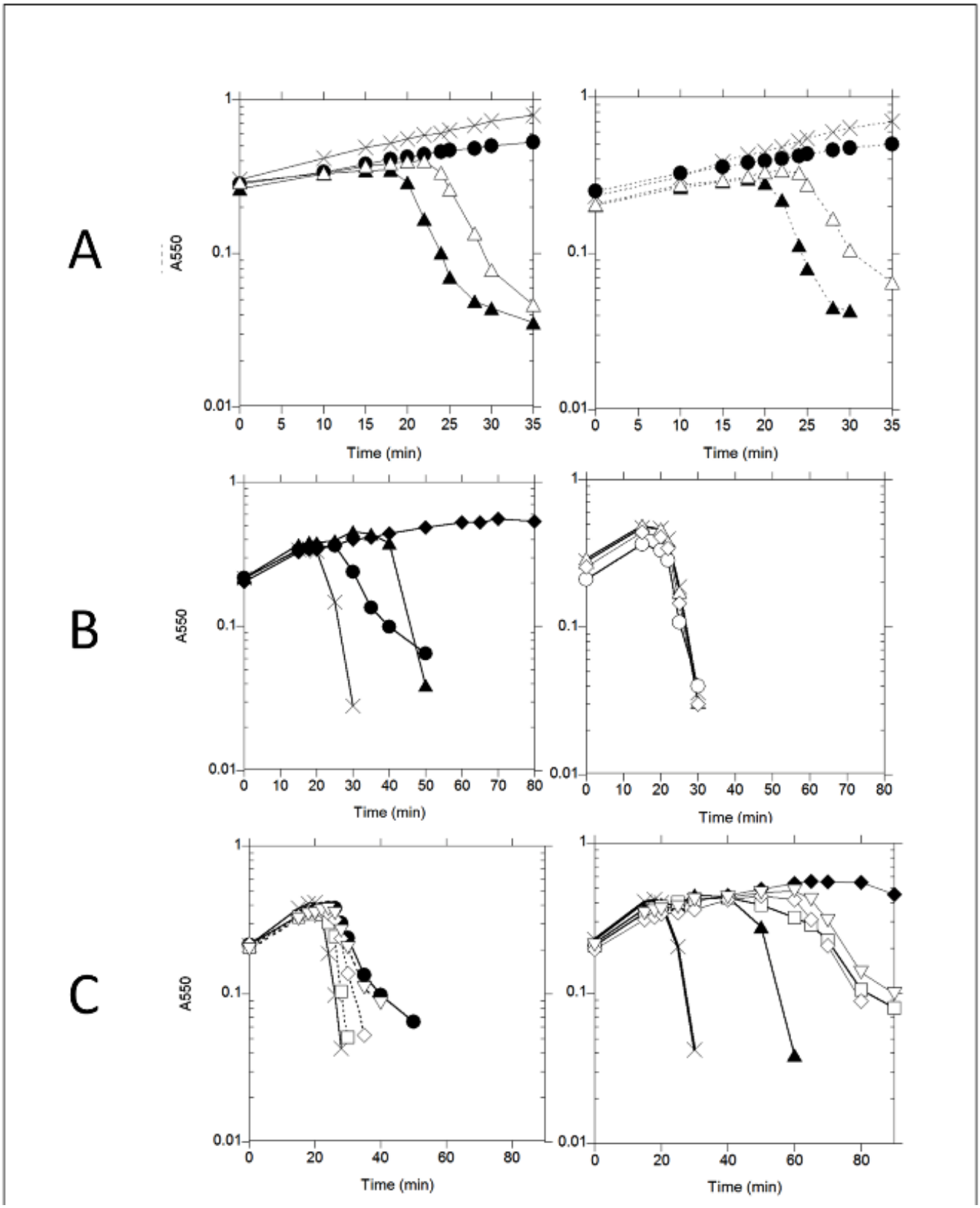

Figure 4

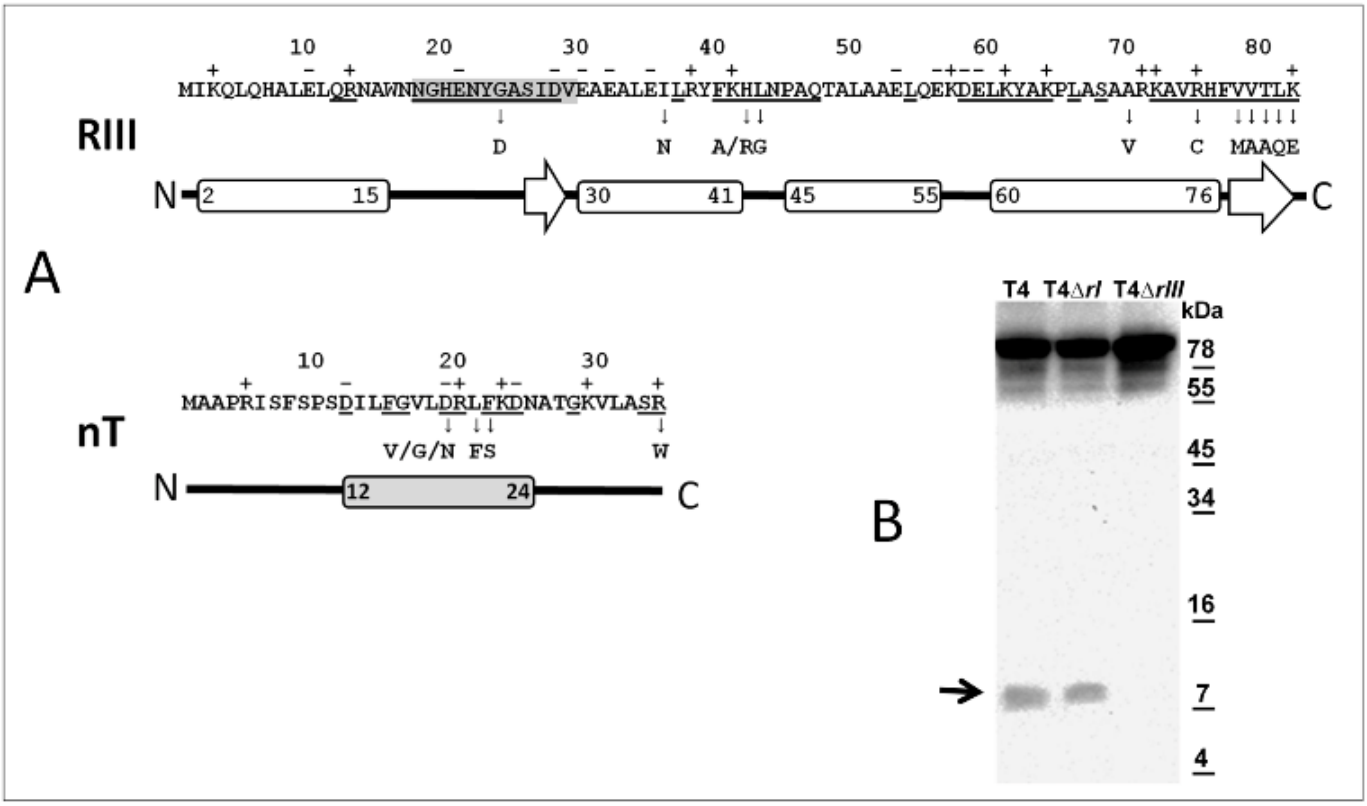

Figure 5

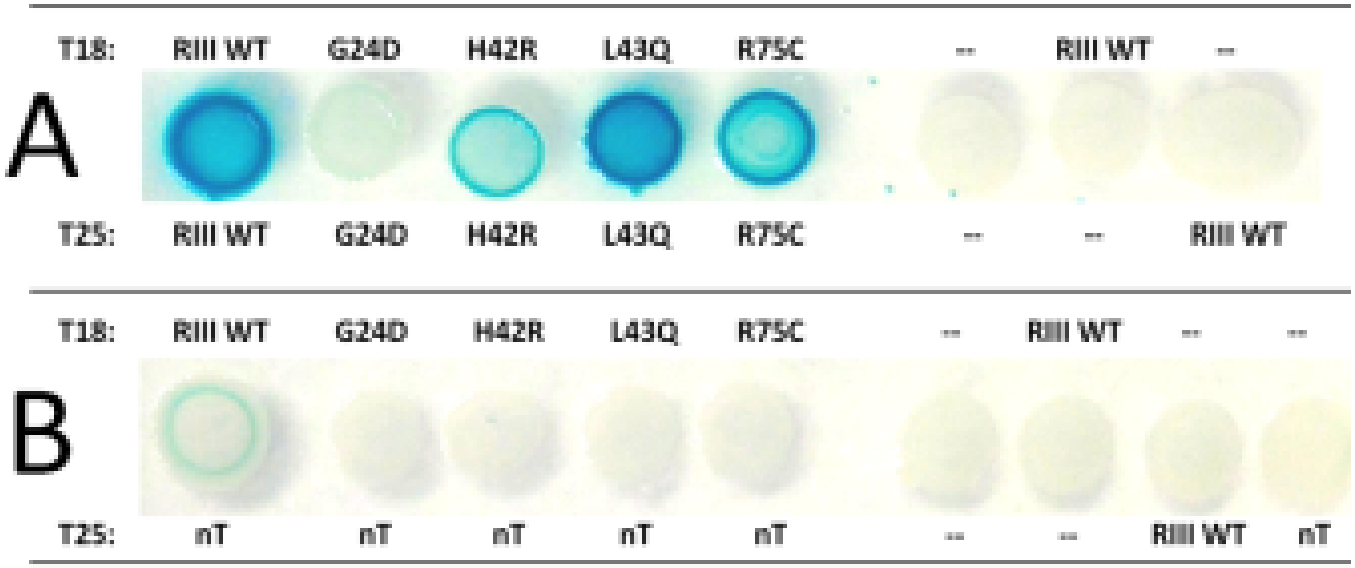

Figure 6

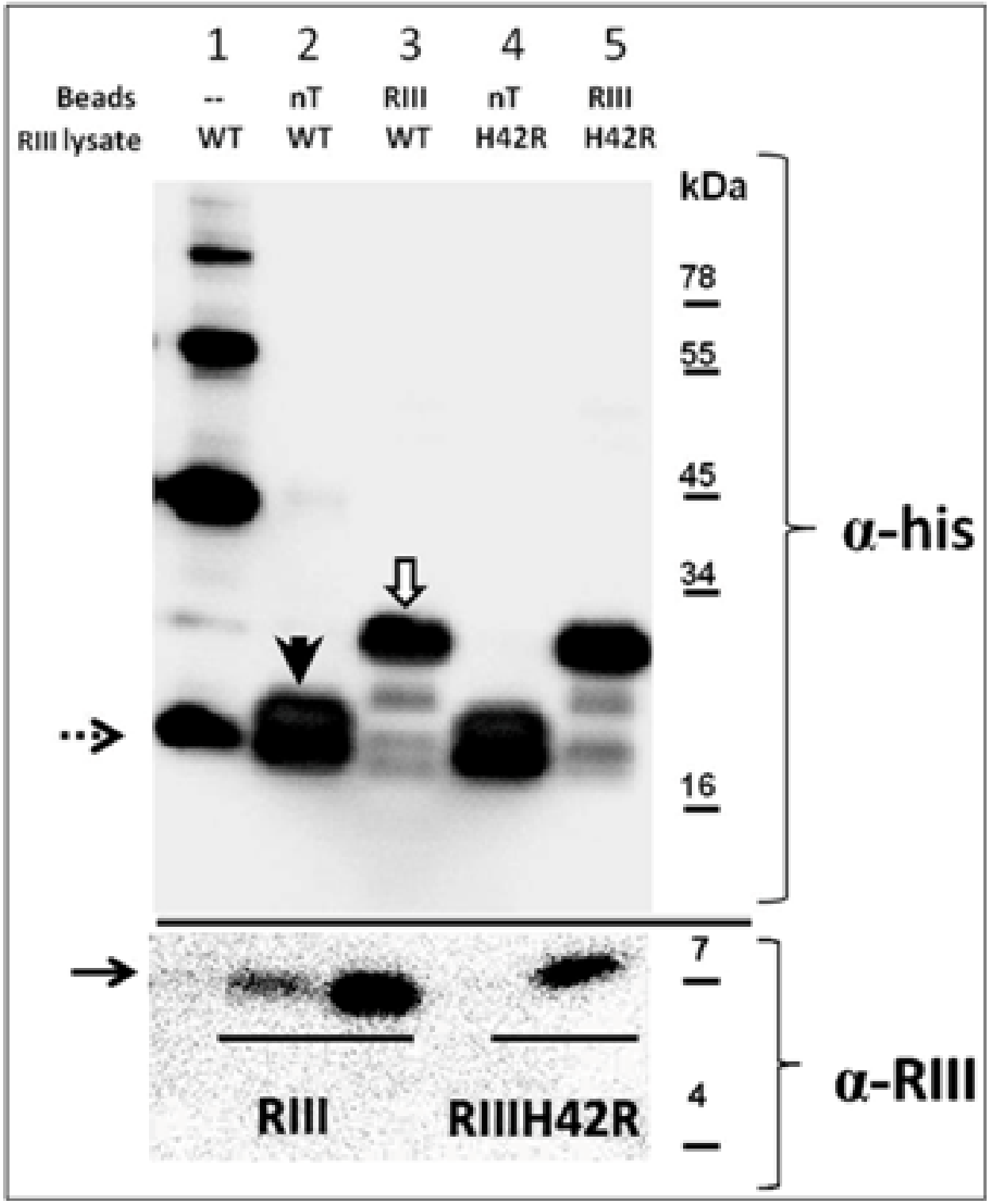

Figure 7

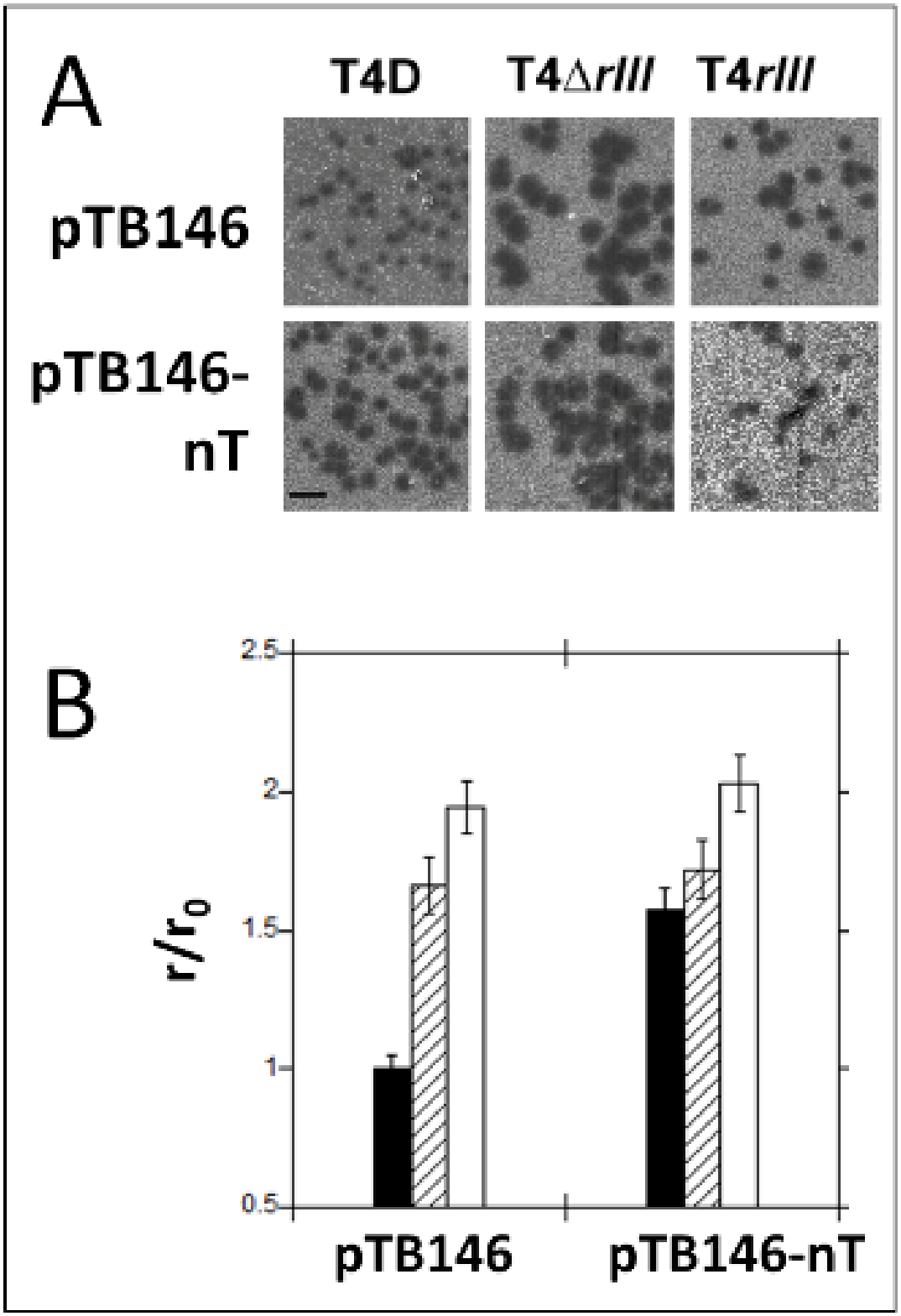

Figure 8